



Special Feature: Nano Structured Devices

Research Report

Design and Application of a Microwave Phase Shifter Based on a Nanomechanical Resonator

Hiroya Tanaka, Takashi Ozaki, Tatsuya Nobunaga, Yutaka Ohno and Yukihiro Tadokoro

Report received on Jul. 3, 2019

■**ABSTRACT**■ Phase shifters are vital components to improve the efficiency of communication systems. We present a theoretical design of an adaptive microwave phase shifter based on a nanomechanical resonator. The phase shifter provides an arbitrary phase rotation in the range from -90° to $+90^\circ$ by tuning the applied bias voltage. We develop an analytical model to comprehend the underlying mechanism of the phase shifter. Further, we propose an antenna array system as an application of the phase shifter. This linear array allows angular sensitivity design in terms of the geometrical properties of the cantilevers, i.e., the array factor can be tuned by the resonant frequency and the distance between the electrode and the tip of the cantilever.

■**KEYWORDS**■ Mechanical Resonators, Nanoelectromechanical Systems (NEMS), Phase Shifter, Antenna Array, Field Emission Current

1. Introduction

Nanomechanical resonators consisting of carbon-based membrane and cantilever have garnered increasing interest in the field of the nanoelectromechanical systems (NEMS) due to their unique attributes, such as high quality factor and high modulus of rigidity.^(1,2) In particular, remarkable efforts have been undertaken for the development of microwave and optical devices, such as sensors,⁽³⁻⁵⁾ switches,⁽⁶⁻⁹⁾ and oscillators,^(10,11) etc. These resonators have demonstrated potential application in both fundamental as well as advanced technologies including wireless networks⁽¹²⁾ and computers.⁽¹³⁾

Distinctive advantages of the nanomechanical resonators include their applications in parallel processing and direct coupling between the electromagnetic/acoustic wave and the resonator.⁽¹⁴⁾ For example, the construction of a functional radio receiver from a carbon nanotube (CNT) cantilever has been reported.⁽⁵⁾ Here, mechanical vibration was excited by the coupling between the incoming radio wave and the charged cantilever. The input signals were then detected from the current emitted at the tip of the CNT. The reception signal was obtained by a parallel processing of the detection, amplification, and demodulation *via* vibration measurements. Moreover, the nanomechanical resonators have also

been used to manipulate the signal of microwave antennas.^(15,16) In particular, the angular sensitivity was controlled by tuning the vibration frequency of the cantilever.⁽¹⁵⁾

Tunable electric devices such as the adaptive filters, phase lock loops, and parametric amplifiers are the building blocks of the next generation communication systems such as cognitive radios⁽¹⁷⁾ and Internet of Things (IoT).⁽¹⁸⁾ Particularly, the phase shifter is a key component because it facilitates the tuning of the relative phase with a microwave signal (analog signal processing), thereby enhancing the performance of the communication systems.^(19,20) However, miniaturization of the modules is a fundamental challenge, particularly if the frequencies are in the kHz or MHz range. This is because the module size should be comparable to the wavelength of the electromagnetic wave. To this end, design of nanometer-scale microwave devices can reduce the size of the entire system.

In this paper, we present a phase shifter composed of a singly clamped CNT mechanical resonator. The bias voltage, which causes the emission of current from the cantilever tip, is used as a tuning parameter for the relative phase. Further, we have developed an analytic model to gain physical insights into the underlying mechanism of the phase shifter. Furthermore, we have theoretically demonstrated that it is possible to achieve

a relative phase shift ranging from -90° to $+90^\circ$ with this device. Finally, a linear antenna array is proposed as an important application of the phase shifter.

2. Methods

2.1 Phase Shifter

We have recently elucidated the mechanism of a phase shifter based on a nanomechanical resonator.⁽²¹⁾ **Figure 1(a)** shows a block diagram of the phase shifter, where the input signal is denoted as s_{in} . The dynamics of the system can be expressed as $s_{out} = h(\omega)s_{in}$, where ω , s_{out} , and $h(\omega)$ are the angular frequency, output signal, and the response of the phase shifter, respectively.

Figure 1(b) shows the schematic configuration of the proposed phase shifter. CNT cantilever of length L is singly clamped on the cathode. A bias voltage V_{ext} is applied between the anode and cathode. This bias voltage induces a charge q at the tip of the cantilever. Voltage $v_e = V_{dc} + v_{ac}$ is applied between the electrodes A and A' at a plate distance d , where V_{dc} and $v_{ac} = s_{in} = V_{ac} \exp(j\omega t)$ are the dc and ac components, respectively. Electric field $e (= v_e/d)$ is created at the

charged tip of the cantilever. This tip is subjected to a y-directional force $F_y = eq$ due to the Coulomb interaction between the induced charge q and electric field e . This results in a physical vibration of the cantilever. As the current is a function of the mechanical vibration, these vibrations can be measured in terms of the current i_{fe} at the detector, which is subjected to the field emission from the cantilever tip.

The motion of the cantilever tip in the y direction can be modeled as the mass-damper-spring system:

$$m\ddot{y} + \eta\dot{y} + ky = qe, \quad (1)$$

where m , η , and k are the effective mass, damping constant, and spring constant of the cantilever, respectively. Solving Eq. (1), the steady-state motion of the tip can be expressed as $y = A_{dc} + A_{ac} \exp[j(\omega t + \phi)]$. Here, the dc and ac amplitudes, A_{dc} and A_{ac} , and the relative phase, ϕ , are expressed as $A_{dc} = qV_{dc}/(kd)$, $A_{ac} = qV_{ac}/[md\sqrt{(\omega^2 - \omega_0^2)^2 + (\omega\omega_0/Q_0)^2}]$, and $\phi = \tan^{-1}[Q_0(\omega_0/\omega - \omega/\omega_0)]$, respectively, where $\omega_0 = \sqrt{k/m}$ and $Q_0 = m\omega_0/\eta$ are the angular resonant frequency and quality factor, respectively. The field emission current is expressed as $i_{fe}(x) = c_1 S E_s^2(x) \exp(-c_2/E_s(x))$, where S is the area of the emitting surface of CNT and E_s is the local electric field in the vicinity of this surface.⁽²²⁾ Here, $c_1 = 3.4 \times 10^{-5} \text{ A/V}^2$ and $c_2 = 7.0 \times 10^{10} \text{ V/m}$ are constants.⁽³⁾ Using first-order expansion and $\Delta x \approx y^2/(2L)$, the ac component of the field emission current can be simplified as $I_{ac} \exp[j(\omega t + \phi)]$, where $I_{ac} = (A_{dc}A_{ac}/L)(\partial I(\Delta x)/\partial y)$. Therefore, the response can be expressed as $h = s_{out}/s_{in} = gI_{ac} \exp(j\phi)$, where g is the amplification gain at the output of the phase shifter. More specifically, the relative phase between the input and output signals is $\arg(h) = \phi = \tan^{-1}[Q_0(\omega_0/\omega - \omega/\omega_0)]$. This suggests that the relative phase can be controlled by tuning the resonant frequency ω_0 , which is a function of the spring constant k .

The effective mass and the spring constant can be expressed as:⁽²²⁾

$$m = 0.250L\rho, \quad (2a)$$

$$k = 2.753 \frac{EI}{L^3} + 1.162 \frac{F_x}{L}. \quad (2b)$$

Notably, the spring constant k is a function of the tensile force (F_x) in the x direction, which is applied

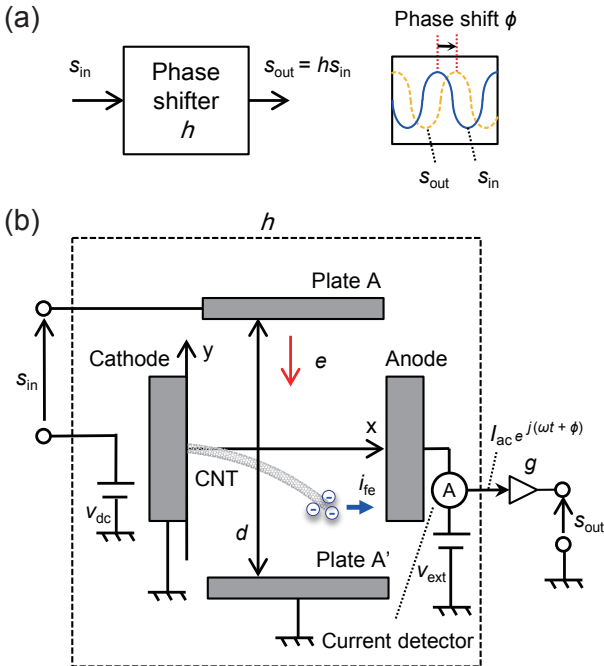


Fig. 1 Schematic of (a) transmission through the phase shifter and (b) a phase shifter based on a nanomechanical cantilever.

to the cantilever tip. Moreover, this tensile force is controlled by the Coulomb interaction between the charges induced at the cantilever tip and the anode. This implies that the resonant frequency ω_0 can be tuned with the bias voltage V_{ext} . Consequently, the relative phase ϕ can be controlled with V_{ext} .

2.2 Design of an Antenna Array Based on the Proposed Phase Shifter

Figure 2 shows a linear array of electromagnetic (EM) wave detectors based on nanomechanical resonators.⁽¹⁶⁾ N elements are linearly placed at a uniform spacing D along the u axis. These elements are composed of multiple CNT cantilevers, which are singly clamped on the cathode. A current detector and bias voltage source is placed between the anode and the cathode. G is a gap length between the anode and the CNT tip. When a radio wave of electric field intensity E_i is applied at an angle θ , it exerts a Coulomb force on the CNT tips due to the interaction between the electric field $E_i \cos\theta \exp(j\omega t)$ and induced charges q . This causes a mechanical vibration of the CNT tips, where the amplitude of the variation is a function of the electric field $E_i \exp(j\omega t)$. As discussed in Sec. 2.1, this vibration can be measured in terms of an output signal s_n ($n = 1, \dots, N$) generated at the current detector. Throughout the band pass filter (BPF), signals $s_{b,n}$ are combined, and eventually signal s_{a0} is observed at

a system frontend.

Using the pattern multiplication principle, the angular sensitivity $P(\theta)$ can be expressed as $A(\theta)K(\theta)$, where A and K are the array factor and the element angular sensitivity, respectively. The element sensitivity is defined as $K(\theta) = \cos^2\theta$.⁽²³⁾ The amplitude and phase of the output signals at each element are governed by the geometrical characteristics of CNT cantilever. This implies that the array factor A can be appropriately designed on the basis of the geometrical characteristics of CNT cantilevers. This factor is expressed as

$$A(\theta) = \sum_{n=0}^{N-1} a_n \exp(2\xi_n) \exp(\Psi_n), \quad (3a)$$

$$a_n = \frac{1}{2LI_0} \left(\frac{\partial i_{fe}}{\partial z} \right) \left(\frac{\left(\frac{q_n E_i}{m} \right)^2}{(\omega^2 - \omega_{0,n}^2)^2 + \left(\frac{\omega \omega_{0,n}}{Q_0} \right)^2} \right), \quad (3b)$$

$$\Psi_n = 2 \tan^{-1} \left[Q_0 \left(\frac{\omega_{0,n}}{\omega} - \frac{\omega}{\omega_{0,n}} \right) \right], \quad (3c)$$

where a_n and Ψ_n are the amplitude and phase rotation of the array factor, respectively. Note that amplitude a_n is normalized with a value I_0 to be $a_n = 1$ at maximum. It is evident from the above equations that a_n and Ψ_n depend on the mechanical properties of the EM wave detector.

3. Results and Discussion

3.1 Tunability of the Phase Shifter

The tunability of the phase shifter can be assessed by observing the variation of phase rotation at different bias voltages (Fig. 3). Here, the resonant frequency is 90 MHz. It is clear that the relative phase varies between -90° to 90° . Inset of Fig. 3 shows the variation of the spring constant with bias voltage. This indicates that both the phase of the input signal s_{in} and the variation of the spring constant can be controlled with the bias voltage.

We analyzed the bandwidth of phase shifter to gain further insights. Figure 4(a) shows that the bandwidth depends on the quality factor of the cantilever. Bandwidth is inversely proportional to the the quality factor (dashed line, $Q_0 = 200$ versus solid

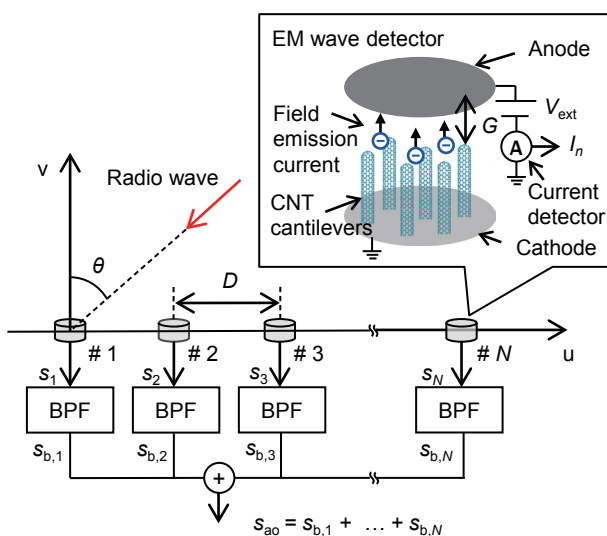


Fig. 2 Schematic of the linear array of EM wave detectors based on the CNT mechanical resonator.

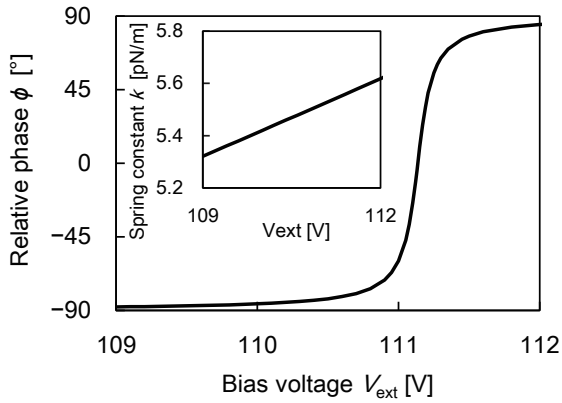


Fig. 3 Tunability of the relative phase ϕ . The spring constant is plotted in the inset. The parameters considered are as follows: the permittivity of free space $\epsilon_0 = 8.854 \times 10^{-12}$ F/m, $V_{dc}/\xi = 0.2$ mV, $V_{ac}/\xi = 0.2$ mV, $d = 1$ μm , $\omega_0/(2\pi) = 90$ MHz, $Q_0 = 700$, $S = 1$ nm^2 , the gap length between the anode and the CNT tip $G = 50$ nm, $\rho = 2160$ kg/m^3 , outer radius $d_o = 5$ nm, inner radius $d_i = 3.5$ nm, $E = 1$ TPa and $L = 800$ nm.

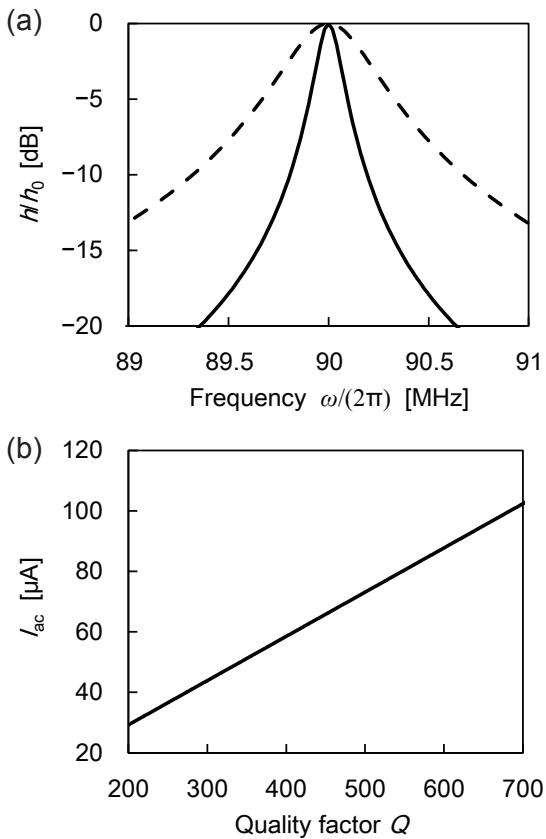


Fig. 4 (a) Normalized amplitude of response (solid line: $Q_0 = 700$, dashed line: $Q_0 = 200$). The amplitude is normalized by h_0 , which is the response at the resonance frequency $\omega_0/(2\pi) = 90$ MHz. (b) Amplitude of AC current I_{ac} . The remaining parameters are same as in Fig. 3.

line, $Q_0 = 700$). However, there is a tradeoff between the bandwidth and the field emission current. This can be verified from Fig. 4(b), where it is observed that the ac field emission current is linearly proportional to the quality factor. It is important to note that the current cannot be measured for small quality factors due to negligible vibration of the cantilever. Therefore, output amplification, i.e. a suitable gain g , is necessary to increase the output signal strength.

3.2 Angular Sensitivity of the Antenna Array

Figures 5(a) and 6(a) show the array factor A and the angular sensitivity P in the uv plane, where appropriate

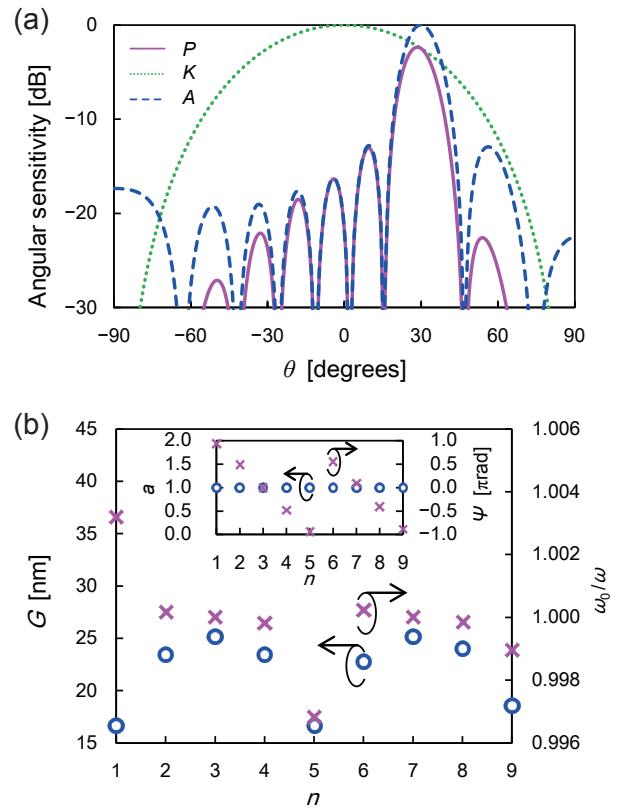


Fig. 5 (a) Angular sensitivity and (b) geometrical properties (circles: gap length G , cross symbols: resonant frequency ω_0) in a setup that allows combination the radio waves with equal amplitudes and phases from $\theta = 30^\circ$. Here, $\epsilon_0 = 8.854 \times 10^{-12}$ F/m, $V_{ext} = 150$ V, CNT radius $\rho = 15$ nm, $E_i = 70$ V/m, $m = 1.5 \times 10^{-19}$ g, $h = 200$ nm, $\omega_0 = 80$ MHz, $Q_0 = 2500$, $S = \pi \times 10^{-18}$ m^2 , $D = 0.9$ m, $M = 100$ and $N = 9$. The amplitude a (circles) and phase rotation Ψ (crosses) of the array factor are plotted in the inset. The amplitude of the array factor is normalized by $I_0 = 0.4$ mA.

values of G and ω_0 are selected for each element, which are shown in Figs. 5(b) and 6(b), respectively. It is evident that the array factor (defined in Eq. (3a)) is steered to $\theta = 30^\circ$ and $\theta = -45^\circ$ (blue dashed lines) depending on the mechanical properties of the CNT cantilever. In addition, P is maximized at $\theta = 29.7^\circ$ and $\theta = -42.3^\circ$ (pink solid lines). The variation of the element pattern K (green dotted line) indicates that an appropriately designed linear array facilitates the spatial filtering of the radio wave.

It is important to note that the proposed linear array design of CNT-based EM wave detectors facilitates angular sensitivity as well, i.e., the signals can be combined with the array factor as the weighing coefficients as expressed in Eqs. (3a)-(3c). For example, in Figs. 5(a) and 6(a), the signals arriving at $\theta = 30^\circ$

and $\theta = -45^\circ$ are combined with equal amplitudes and phases according to the weights shown in the inset of Figs. 5(b) and 6(b), $a_n = 1$ and $\Psi_n = -2\xi_n$. Further, we emphasize that such an array factor is determined by the mechanical properties of the EM wave detectors, i.e., the gap length G and the resonant frequency ω_0 , as shown in Figs. 5(b) and 6(b). This is fundamentally different from the conventional analog array antennas where the array factor design requires additional microwave components such as gain controllers and phase shifters.

4. Conclusion

We have proposed a phase shifter based on a nanomechanical resonator, which utilizes the current emitted from the cantilever tip. This is complemented by an analytical model that provides useful insights into the detailed mechanism of the phase shifter. This model harnesses the effect of the tensile force on the cantilever tip and the relative phase of the vibration. A significant outcome is that the relative phase ranging from -90° to $+90^\circ$ can be achieved by varying the bias voltage. Further, we demonstrate that the quality factor plays a pivotal role in the bandwidth of the phase shifter. Furthermore, we have developed an antenna array of EM wave detectors, comprising CNT-based nanomechanical resonators. Notably, the array factor is designed by tuning the mechanical properties, i.e., resonant frequency of the cantilever and gap length between the anode and CNT tip. This indicates that CNT-based EM wave detectors can tune the array factor without additional electrical components such as phase shifters and gain controllers, which is a crucial requirement in the conventional array antennas.

Acknowledgments

We thank Prof. J. Hirotsu for fruitful discussions about fabrications of CNT. Discussions with Mr. K. Funayama has been also helpful to us.

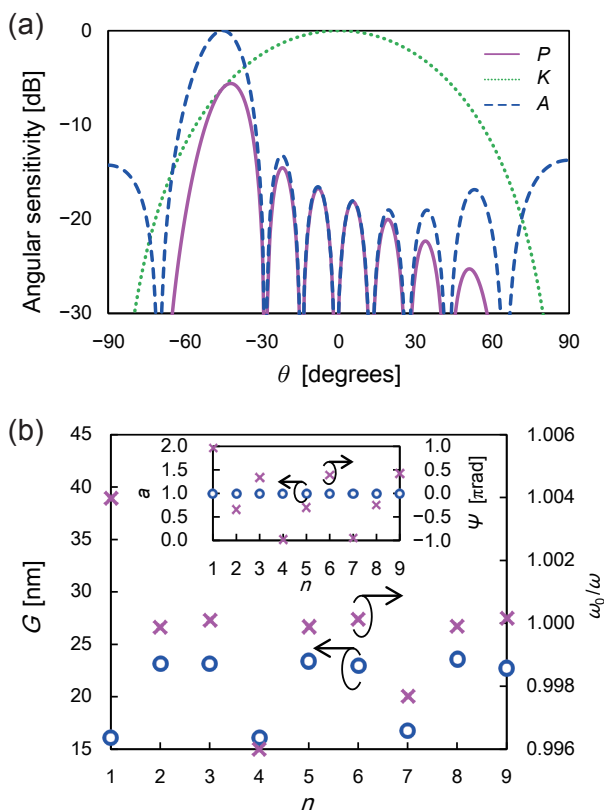


Fig. 6 (a) Angular sensitivity and (b) geometrical properties (circles: gap length G , cross symbols: resonant frequency ω_0) in a setup that allows combination of the radio waves with equal amplitudes and phases from $\theta = -45^\circ$. The amplitude a (circles) and phase rotation Ψ (crosses) of the array factor are plotted in the inset. The remaining parameters (apart from G and ω_0) are same as in Fig. 5.

References

- (1) Bunch, J. S., Van der Zande, A. M., Verbridge, S. S., Frank, I. W., Tanenbaum, D. M., Parpia, J. M., Craighead, H. G. and McEuen, P. L., *Science*, Vol. 315, No. 5811 (2007), pp. 490-493.
- (2) Li, M., Tang, H. X. and Roukes, M. L., *Nat. Nanotechnol.*, Vol. 2 (2007), pp. 114-120.
- (3) Jensen, K., Weldon, J., Garcia, H. and Zettl, A., *Nano Lett.*, Vol. 7, No. 11 (2007), pp. 3508-3511.
- (4) Jensen, K., Kim, K. and Zettl, A., *Nat. Nanotechnol.*, Vol. 3 (2008), pp. 533-537.
- (5) Willick, K., Haapamaki, C. and Baugh, J., *J. Appl. Phys.*, Vol. 115, No. 11 (2014), 114501.
- (6) Acquaviva, D., Arun, A., Esconjauregui, S., Bouvet, D., Robertson, J., Smajda, R., Magrez, A., Forro, L. and Ionescu, A. M., *Appl. Phys. Lett.*, Vol. 97, No. 23 (2010), 233508.
- (7) Chen, Z., Tong, L., Wu, Z. and Liu, Z., *Appl. Phys. Lett.*, Vol. 92, No. 10 (2008), 103116.
- (8) Li, P., You, Z. and Cui, T., *Appl. Phys. Lett.*, Vol. 101, No. 9 (2012), 093111.
- (9) Chakraborty, R. S., Narasimhan, S. and Bhunia, S., *IEEE Trans. Circuits Syst. I: Regul. Pap.*, Vol. 54, No. 11 (2007), pp. 2480-2488.
- (10) Chen, C., Lee, S., Deshpande, V. V., Lee, G.-H., Lekas, M., Shepard, K. and Hone, J., *Nat. Nanotechnol.*, Vol. 8 (2013), pp. 923-927.
- (11) Jeong, B.-W. and Sinnott, S. B., *Appl. Phys. Lett.*, Vol. 95, No. 8 (2009), 083112.
- (12) Mahboob, I., Okamoto, H. and Yamaguchi, H., *Sci. Adv.*, Vol. 2, No. 6 (2016), 1600236.
- (13) Akyildiz, I. F. and Jornet, J. M., *Nano Commun. Netw.*, Vol. 1, No. 1 (2010), pp. 3-19.
- (14) Dykman, M. I., *Fluctuating Nonlinear Oscillators: From Nanomechanics to Quantum Superconducting Circuits* (2012), 432p., Oxford University Press.
- (15) Tanaka, H., Ohno, Y. and Tadokoro, Y., *IEEE Trans. Mol. Biol. Multi-scale Commun.*, Vol. 3, No. 1 (2017), pp. 24-32.
- (16) Nobunaga, T., Tadokoro, Y., Ohno, Y. and Tanaka, H., *IEEE Antennas Wireless Propag. Lett.*, Vol. 16 (2017), pp. 1405-1408.
- (17) Wang, B. and Liu, K. J. R., *IEEE J. Sel. Topics Signal Process.*, Vol. 5, No. 1 (2011), pp. 5-23.
- (18) Yedavalli, P. S., Riihonen, T., Wang, X. and Rabaey, J. M., *IEEE Access*, Vol. 5 (2017), pp. 1743 -1752.
- (19) Abbosh, A. M., *IEEE Trans. Microwave Theory Tech.*, Vol. 60, No. 8 (2012), pp. 2465-2472.
- (20) Seleem, H., Sulyman, A. I. and Alsanie, A., *IEEE Access*, Vol. 5 (2017), pp. 6813-6823.
- (21) Tanaka, H., Ozaki, T., Ohno, Y. and Tadokoro, Y., *J. Appl. Phys.*, Vol. 122, No. 23 (2017), 234501.
- (22) Fowler, R. H. and Nordheim, L., *Proc. R. Soc. A*, Vol. 119, No. 781 (1928), pp. 173-181.
- (23) Tanaka, H., Ohno, Y. and Tadokoro, Y., *IEEE Trans. Nanotechnol.*, Vol. 14, No. 6 (2015), pp. 1112-1116.

Figs. 1, 3 and 4

Reprinted from *J. Appl. Phys.*, Vol. 122, No. 23 (2017), 234501, Tanaka, H., Ozaki, T., Ohno, Y. and Tadokoro, Y., Phase Shifter Tuned by Varying the Spring Constant of a Nanomechanical Cantilever, © 2017 Authors.

Figs. 2, 5 and 6

Reprinted from *IEEE Antennas Wireless Propag. Lett.*, Vol. 16 (2017), pp. 1405-1408, Nobunaga, T., Tadokoro, Y., Ohno, Y. and Tanaka, H., Angular Sensitivity Steering in CNT Electromagnetic Wave Detector, © 2016 IEEE, with permission from IEEE.

Hiroya Tanaka

Research Fields:

- Nonlinear Signal Processing Exploiting Noise
- Nanomechanical Systems for Signal Processing
- Wireless Communications
- Applied Radio Instrumentation and Measurements

Academic Degree: Dr.Eng.

Academic Society:

- IEEE Microwave Theory and Techniques Society

Award:

- Telecom System Technology Award, The Telecommunication Advancement Foundation, 2017



Takashi Ozaki

Research Fields:

- Bioinspired Actuators and Robotics
- Micro Electromechanical Systems
- Microfabrication Processes



Tatsuya Nobunaga

Research Fields:

- Biomedical Signal Processing
- Machine Learning and Statistical Signal Processing
- Sensor Systems and Circuits

Academic Society:

- The Institute of Electronics, Information and Communication Engineers

Award:

- Young Researcher's Award, Engineering Sciences Society, IEICE, 2017



Yutaka Ohno*

Research Field:

- Low-dimensional Materials and Their Electronics Applications

Academic Degree: Ph.D.

Academic Societies:

- The Japan Society of Applied Physics
- The Institute of Electronics, Information and Communication Engineers
- The Fullerenes and Nanotubes Research Society
- American Chemical Society
- Material Research Society

Awards:

- Lee Hsun Research Award, Institute of Metal Research, Chinese Academy of Sciences, 2019
- Academic Award, The NAGAI Foundation for Science & Technology, 2016
- APEX/JJAP Editorial Contribution Award, The Japan Society of Applied Physics, 2012



Yukihiro Tadokoro

Research Fields:

- Nonlinear Signal Processing Exploiting Noise
- Nanomechanical Systems for Signal Processing
- Wireless Communications

Academic Degree: Dr.Eng.

Academic Societies:

- IEEE Nanotechnology Council
- IEICE NOLTA Society

Award:

- Telecom System Technology Award, The Telecommunication Advancement Foundation, 2017



*Nagoya University